Jurnal Teknologi

Full Paper

WETTABILITY AND SURFACE ENERGY BEHAVIOR OF GRAPHENE QUANTUM DOTS CONCENTRATIONS

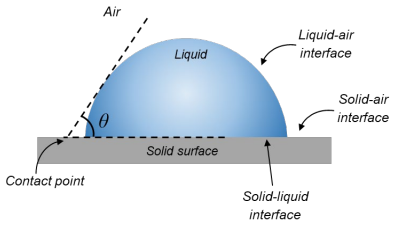
Aida Zulia Zulhanip[a], Nor Shahanim Mohamad Hadis[a]*, Afaf Rozan Mohd Radzol[a], Zurita Zulkifli[b], Anis Diyana Rosli[a],

[a]Electrical Engineering Studies, College of Engineering, Universiti Teknologi MARA, Pulau Pinang Branch, 13500 Permatang Pauh, Pulau Pinang, Malaysia
[b]School of Electrical Engineering, College of Engineering, Universiti Teknologi MARA, 40450 Shah Alam, Selangor Darul Ehsan, Malaysia

Article history
Received
21st January 2025
Received in revised form
1st January 2026
Accepted
18th February 2026
Published
1st November 2026

*Corresponding author
norsh713@uitm.edu.my

Graphical abstract



Abstract

Graphene Quantum Dots (GQDs) were used in various fields including coating, biomedical devices, and sensing. The production of hydrophilic GQDs is indisputable due to the oxygenated functional groups, which effectively enhance the aqueous solubility. This study investigates the effects of different GQDs concentrations on the wettability and surface energy of thin film GQDs. The GQDs were initially prepared using hydrothermal synthesis from different concentrations of sodium hydroxide (NaOH) and were deposited onto substrate using drop-casting method to form thin film GQDs. The contact angles were measured through the water droplet to evaluate wettability and performed zeta potential analysis to assess colloidal stability. Young's Dupré equation was employed to measure the surface energy through the work of adhesion between test liquid and solid substrate, and FTIR analysis used to recognize the functional group contributing to the observed trends. The finding reveals a significant dependence of wettability on GQDs concentration. Lower concentrations of GQDs (GQDs1 and GQDs2) resulted in a hydrophilic surface property of contact angles (62.83°, 66.57°). However, higher concentrations of GQDs (GQDs3 and GQDs4) exhibited enhanced hydrophilicity as reflected by the reduced contact angles (36.43°, 36.83°) with stronger solid-liquid adhesion, W_{SL} (131.07 mN/m, 131.37 mN/m). Higher concentrations of GQDs demonstrate good dispersion stability as evidenced by zeta potential measurement. FTIR analysis highlighted the irregular interrelation between the GQDs functional group and their influence on contact angle and stability. This study offers insights into tailoring GQD thin films for sensing and surface engineering applications, particularly in controlling and enhancing wettability.

***Keywords*:** Graphene Quantum Dots (GQDs), Wettability, Contact Angle, Zeta Potential, Fourier Transform Infrared Spectroscopy (FTIR).

DOI: https://doi.org/10.11113/jurnalteknologi.v89.24216

Abstrak

Titik Kuantum Graphene (GQDs) telah digunakan dalam pelbagai bidang, termasuk salutan, peranti bioperubatan dan penderiaan. Penghasilan GQDs hidrofilik tidak dapat dipertikaikan kerana kumpulan berfungsi beroksigen, yang secara berkesan meningkatkan keterlarutan dalam air. Kajian ini menyiasat kesan kepekatan GQDs yang berbeza terhadap kebasahan dan tenaga permukaan filem nipis GQDs. GQDs pada mulanya disediakan menggunakan sintesis hidroterma daripada kepekatan natrium hidroksida (NaOH) yang berbeza dan didepositkan ke atas substrat menggunakan kaedah tuangan titisan untuk membentuk filem nipis GQDs. Sudut sentuhan diukur melalui titisan air untuk menilai kebasahan dan analisis potensi zeta dilakukan untuk menilai kestabilan koloid. Persamaan Young-Dupré digunakan untuk mengukur tenaga permukaan melalui kerja lekatan antara cecair ujian dan substrat pepejal, dan analisis FTIR digunakan untuk mengenali kumpulan berfungsi yang menyumbang kepada trend yang diperhatikan. Penemuan telah menunjukkan pergantungan ketara kebasahan pada kepekatan GQDs. Kepekatan GQDs yang lebih rendah (GQDs1 dan GQDs2) menghasilkan sifat permukaan hidrofilik dengan sudut sentuh (62.83°, 66.57°). Walau bagaimanapun, kepekatan GQD yang lebih tinggi (GQDs3 dan GQDs4) menunjukkan hidrofilik yang lebih baik seperti yang tertera melalui pengurangan sudut sentuh (36.43°, 36.83°) dengan lekatan pepejal-cecair yang lebih kuat, W_{SL} (131.07 mN/m, 131.37 mN/m). Kepekatan GQDs yang lebih tinggi menunjukkan kestabilan penyebaran yang baik seperti yang dibuktikan oleh pengukuran potensi zeta. Analisis FTIR memperlihatkan hubungan yang tidak teratur antara kumpulan fungsi GQDs dan pengaruhnya terhadap sudut sentuh serta kestabilan. Kajian ini menawarkan penilaian untuk menyesuaikan filem nipis GQDs bagi aplikasi penderiaan dan kejuruteraan permukaan, terutamanya dalam mengawal dan meningkatkan kebasahan.

Kata kunci: Titik Kuantum Grafena (GQDs), Kebasahan, Sudut Sentuh, Potensi Zeta, Spektroskopi Inframerah Transformasi Fourier (FTIR)

©2026 Penerbit UTM Press. All rights reserved

1.0 INTRODUCTION

In recent years, a rapidly increasing interest in graphene quantum dots (GQDs) in the scientific and industrial community has built on earlier enthusiasm for two-dimensional graphene and three-dimensional carbon nanotubes. Researchers have already recognized Graphene Quantum Dots (GQDs) as hydrophilic. Hydrophilic GQDs with oxygenated functional groups such as hydroxyl, carboxyl, and epoxy groups ensure excellent solubility and stability in water, making them desirable for biological and environmental applications. Their hydrophilic nature of GQDs effectively improves the aqueous solution, simple, high sensitivity and suitable for sensing material [1], biomedical devices [2], and incorporation as coatings to enhance performance in specific applications [3], [4], [5].

The materials division usually conducts the analysis of solubility in GQDs materials. GQDs that present solubility in water, lipids, and proteins possess hydrophilic characteristics [6], [7] and are categorized as organic compounds. The hydrophobic nature, alternatively, concentrates on organic solvents solutions [8] and has its molecules mainly composed of hydrophobic groups. The classification of offered GQDs was presented to achieve an increased and optimized hydrophilic nature. It has given the diversity and application potential of GQDs essentially to explore the differences, characteristics, performances, and applications of these particles in diverse areas, especially in the absorption and removal of contaminants in water.

Contact angle is a quantitative measure used to indicate the state of hydrophilic (surface wettability) or hydrophobic (non-wettability) surface. The angle symbolized as θ, between the liquid-air and liquid-solid interfaces at the three-phase contact point reveals the contact angle measurement that led to the indicator of hydrophilic and hydrophobic-related studies.

Liquids often interact with solid surfaces, and this physical phenomenon is called wettability. The simplest and most convincing evidence for surface wettability is a change in the shape of liquid droplets on a solid surface. Droplets on some surfaces become spherical, while on other surfaces, droplets spread to a thin layer, as shown in Figure 1. Measuring the angle, i.e., the contact angle formed at the periphery of a liquid droplet can provide helpful information about the surface's wettability.

DOI: https://doi.org/10.11113/jurnalteknologi.v89.24216

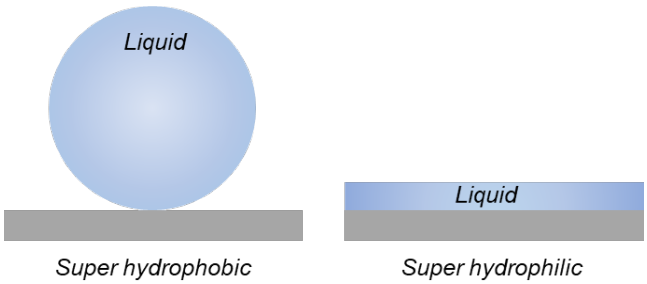


Figure 1 Liquid droplet on a solid surface

Surface wettability is one of the important properties that guide numerous aspects. The information obtained is crucial in providing an in-depth analysis through various applications. According to Jinxin T. et al.'s (2023) study, this work investigates the factors influencing the wettability of various plant leaves. The highlighted factors of the chemical composition, surface microstructure, hierarchical structure, and growth age were discussed, along with the contribution of wetting properties and their impacts on anti-soil properties [9]. At the same time, Chen Z. and co-workers (2024) focused on the implications of adsorption energy and surface electrical charge on contact angle for talc and muscovite mineral surface wettability with computational simulations [10]. The findings of this work reveal the hydrophilic and hydrophobic characteristics of these mineral surfaces as valuable guidelines. The hydrophilicity affinity and hydrophobicity resistance of surface characteristics are reflected by Fourier transform infrared (FTIR) analysis, which helps to identify the functional group present on the material surface since the functional group significantly influences the surface wettability. Nandi V. et al. (2018) explore the utilization of attenuated total reflectance Fourier transform infrared spectroscopy (ATR-FTIR) to understand the wetting transition on superhydrophobic surfaces [11]. This suggests how FTIR assists in comprehending the dynamics of wettability changes related to surface properties. Recent work discusses the different combustion conditions and film thickness that influence the wettability behaviors of carbon nanoparticle coating and the engagement of FTIR to identify the chemical properties of surfaces. This research establishes a correlation between hydrophilic and hydrophobic interactions [12].

Zeta potential is a crucial measurement for appreciating surface properties (e.g., chemical composition, roughness, charge, and wettability) as it provides insight into the magnitude of the electrostatic repulsion or attraction between particles in a medium. While it does not directly measure hydrophilic and hydrophobic behaviors, the zeta potential parameter reflects surface charge, influencing the wettability and colloidal stability [13], [14]. Representative + 30 mV to -30 mV of zeta potential values are recognized as a borderline between stable and unstable suspensions. A value nearer to zero is considered less stable and higher than +/- 30 mV, representing a stable dispersion [15], [16].

1.1 CONTACT ANGLE MEASUREMENT: SESSILE DROP METHOD

The contact angle of a liquid on a specific solid surface is a physical quantity used to elucidate the magnitude to which liquids wet that surface. The ability of a substrate to maintain a certain contact angle dictates whether the surface displays special wettability performances. The numerical values of a substrate's contact angle are used to predict and guide the end-use application of a variety of fluids on various substrates. These have important practical applications ranging from materials designs to industrial procedures that require the formation of complex wettability patterns.

Various methods are available to determine the contact angle for the solid flat base, including sessile drop, trapped bubble, till table, drop profile, and Wilhelmy method [17][18]. The classical sessile drop method uses an optical goniometer, which is the most used of these methods. The contact angle is a necessary measurement tool for surface characterization and is estimated using the sessile drop method. Two techniques of sessile drop measurements are available: static contact angle and dynamic contact angle measurements. The static contact angle is measured when the liquid droplet does not require any movement from the measurement steps, and its angle is measured using image analysis. The dynamic contact angle can be measured while the droplet is in motion (tilting the surface) to determine the advancing and receding angles [19].

1.2 STATIC CONTACT ANGLE MEASUREMENT

The static contact angle measurement formed when a liquid droplet was placed on a solid surface. This method assesses the surface's wettability and surface energy, defined as the angle between the tangent to the solid surface at the three-phase contact point and the tangent to the liquid-air interface at the same point [20]. Figure 2 illustrates the contact angle, θ of the liquid droplet on a solid surface.

DOI: https://doi.org/10.11113/jurnalteknologi.v89.24216

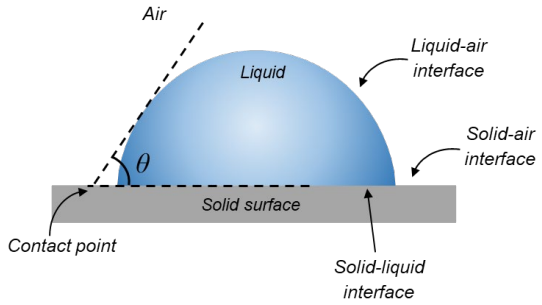


Figure 2 Illustration of a liquid droplet on a solid surface showing the interfacial at three-phase contact point [20].

The contact angle is a robust index in determining surface wettability. Wettability refers to extending the contact angle across the surface materials or solid surface, which is the degree of contact between a liquid and a solid. The experimental contact angle can easily be accessed by dictating the surface's wettability. The relationship between contact angle and the wettability nature is generally accepted on four scales as shown in Table 1 [21].

Table 1: The range of contact angles relative to surface wettability [21].

Angle of Contact angle, θ	Surface wettability
0° < θ < 10°	Super hydrophilic
10°< θ < 90°	Hydrophilic
90°< θ < 150°	Hydrophobic
θ > 150°	Super hydrophobic

The contact angle exhibits a broad spectrum covering the range from 0° to 180°. For decades, solid surfaces were classified as hydrophilic when the contact angle was less than 90° and as hydrophobic when the angle was more significant than 90°. For more complex surfaces, they exhibit super hydrophilic characteristics, which enhance the wettability towards water and reduce the contact angle to less than 10° with the superhydrophobic being greater than 150°. Until now, it has been considered that surface wettability is determined by the intrinsic properties of the material, often dictated by the chemical composition.

In this study, GQDs formation is from the oxygenated functional group, which enhances the aqueous solubility. A base additive of NaOH was used as a reducing agent to exfoliate GO into GQDs. The use of NaOH was crucial in this process as it facilitated the exfoliation of GO into GQDs, thereby influencing their wettability. A varied concentration of NaOH, and the influence of various GQD solutions were investigated by gauging the wettability measured by the contact angle. The stability of GQDs was examined in relation to surface wettability. To our knowledge, no reports regarding the variation in GQD concentrations investigate the contact angle and wettability. Findings from zeta potential and FTIR analysis support this study.

2.0 METHODOLOGY

2.1 MATERIALS

GQDs solution was synthesized from commercially available graphene oxide (GO) powder (15–20 sheets, 4–10% edge oxidized) purchased from Sigma Aldrich. An alkaline additive, sodium hydroxide (NaOH, reagent grade, 97% purity, powder, product no. 655104), was purchased as a base catalyst from Sigma Aldrich to assist the hydrothermal cutting process. Deionized (DI) water was used throughout the experimental procedures to maintain the highest purity standards and minimize contamination.

2.2 GQDs SOLUTION PREPARATION

The supernatant GQDs suspension was synthesized using commercially available graphene oxide (GO) powder. The GO powder was first dissolved in DI water and stirred gently for a few minutes until the GO was uniformly dispersed. The GO colloidal dispersion was treated with sodium hydroxide (NaOH), an alkali additive, to synthesize the pure GQDs without any heteroatom's integration. The NaOH solution was prepared aside and then mixed into the GO suspension. Next, the mixture undergoes a sonication process to ensure uniform mixing. The composition solution was allowed to cool at room temperature before being transferred to a Teflon-lined autoclave and heated at 200 °C for 24 hours. Upon completion of the hydrothermal treatment process, the reaction mixture was subjected to high-speed centrifugation to remove larger agglomerates or any unreacted materials. Eventually, the supernatant GQDs were filtered and further purified through dialysis process overnight to eliminate residual ions. (A. Z. Zulhanip, N.S. M. Hadis, A.F. M. Rozan, Z. Zulkifli, A. D. Rosli, manuscript submitted).

2.3 GQD THIN FILM PREPARATION

The GQD solutions were prepared at several concentrations, known as GQDs1, GQDs2, GQDs3, and GQDs4. Each GQD represented four different NaOH concentrations, and the synthesized GQDs underwent a similar procedure shown in Table 2.

Table 2 GQDs representing NaOH concentrations

Sample	NaOH Concentration (M)	GO Concentration (mg/mL)	Strength description
GQDs1	0.1	0.5	Lowest

DOI: https://doi.org/10.11113/jurnalteknologi.v89.24216

GQDs2	0.5	0.5	Moderate
GQDs3	1.0	0.5	High
GQDs4	1.5	0.5	Strongest

A few drops of GQDs were applied to a clean glass slide via the drop-cast method and left for 48 hours at room temperature for an incubation process. Later, the GQDs/glass slide was baked for 10 minutes at 100 °C to eliminate any residual water and humidity after cleaning with the DI water. This process can improve GQDs film adhesion to the glass slide. Figure 3 illustrates how the prepared GQDs and glass slide substrate are prepared.

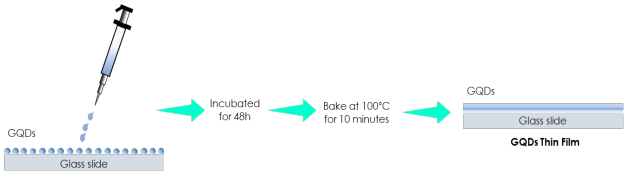


Figure 3 Illustration of GQDs thin film preparation process

2.4 CHARACTERIZATION AND ANALYSIS

The wettability and surface energy analysis of GQDs thin films was measured using a contact angle goniometer, AST/VCA-3000s, as shown in Figure 4. This wafer surface analysis system utilizes a high-resolution video camera to capture static images of the droplets and determine tangent lines for contact angle measurement. The Fourier transform infrared (FTIR) Perkin Elmer Spectrum 400 spectroscopy was used to analyze the surface functional groups of GQDs thin films, and the zeta potential Zen3600 was used to gather information on the colloidal stability and dispersion characteristics of GQDs.

The surface charge and colloidal stability were measured using the zeta potential of different GQDs concentration solutions. 1 mL of each GQD solution was transferred into the designed cuvette and looked out to avoid any air bubbles during sample loading to avoid any interference with the analysis. The process was performed three times per concentration to ensure the measurement's accuracy was repeated. These methods were chosen for their ability to provide accurate and reliable data on the properties of GQDs thin films.

Morphological analysis was conducted via Ultra-high resolution scanning electron microscopy (UHR-SEM) images on a Hitachi Regulus 8220 and the elemental composition using Energy Dispersive X-ray (EDX). The morphology of individual GQDs were characterized using Transmission Electron Microscopy (TEM) images obtained on a Zeiss Libra 120 and the crystalline structure was analyzed with X-ray diffraction (XRD) using the Rigaku Ultima IV system



Figure 4 The contact angle goniometer, AST/VCA-3000s

3.0 RESULTS AND DISCUSSION

3.1 CONTACT ANGLE ANALYSIS

The angle between the droplet and the surface is recorded as the droplet flattens. The sample is placed on the stable and horizontal platform during measurements. A controlled syringe is used to disperse a volume of 1.0 µL of DI water onto the sample. Each droplet volume was carefully controlled to ensure consistency across all measurements. After the test liquid is released from the tube, water spreads and settles on the GQDs/ glass substrate, forming a static contact angle; the high-resolution image captures it immediately. The measurement procedure takes place by arranging the five points (L, R, T, 1, and 2) at the edge of the droplets, as shown in Figure 5.

DOI: https://doi.org/10.11113/jurnalteknologi.v89.24216

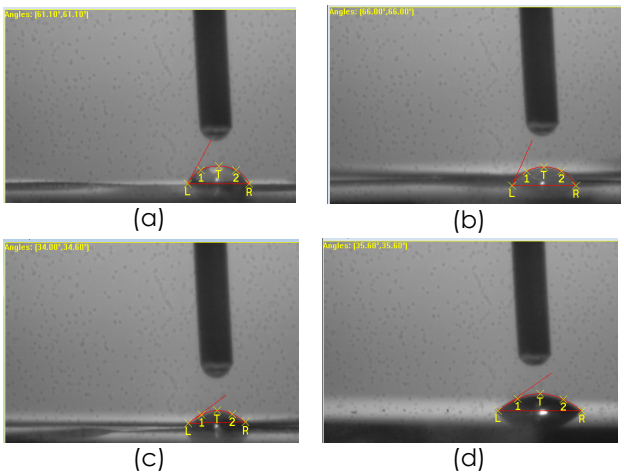


Figure 5 The contact angle measurement of different concentrations (a) GQDs1 (NaOH = 0.1 g/mol), (b) GQDs2 (NaOH = 0.5 g/mol), (c) GQDs3 (NaOH = 1.0 g/mol), (d) GQDs4 (NaOH = 1.5 g/mol).

The images of contact angle measurement for four GQDs concentrations GQDs1, GQDs2, GQDs3 and GQDs4 were presented in Figures 5(a), 5(b), 5(c) and 5(d) respectively. Each point must be accurately arranged, correspond to the outline of the droplet, and can be tracked by the lines surrounding its shape. The reported contact angle values are based on three repeats.

Table 3 shows the mean contact angle, and the standard deviation reflects the measurement for each GQD concentration. Various NaOH concentrations affect the wettability of GQDs, which are characterized by contact angle measurements. The mean contact angle of each GQD concentration appears to be in a group of range 10° < θ < 90°, showing the hydrophilic surface wettability. The GQDs1 (0.1 g/mol) indicated moderate hydrophilic at a contact angle of 62.83° and increasing GQDs2 concentration (0.5 g/mol), suggesting a tendency towards hydrophobicity at 66.57°. However, further increases in NaOH concentration GQDs3 and GQDs4 (1.0 and 1.5 M) demonstrate the transition to a more hydrophilic state with lower contact angles of 36.83° and 36.43°, respectively. From this study, GQDs2 and GQDs4 show the lowest standard deviation, revealing the most consistent wettability among GQDs concentrations. The corresponding contact angle confirms its robustness as a characteristic property of the surface [22].

Table 3 GQDs concentrations measurement of mean contact angle and standard deviation

Sample	Mean Contact Angle (°)	Standard Deviation (°)
GQDs1	62.83	1.86
GQDs2	66.57	1.53
GQDs3	36.83	2.46
GQDs4	36.43	1.44

3.2 SURFACE ENERGY: SOLID-LIQUID ADHESION

With the intentions to understand the surface's wettability, it is essential to understand the interactions between solid surface and liquid adhesion behavior. The interaction between liquid and solid is determined by the intermolecular forces, usually governed by surface free energy, also called surface energy [23]. The surface energy is one of the most important factors for surface effects. The surface energy affects whether a liquid approaching the surface spreads or forms a drop. Both surface energy and contact angle can be calculated and interpreted using many different equations and theories [24], [25].

The Young – Dupré Law states that when a drop of liquid touches the solid surface, there will be a balanced interplay between the work of adhesion between the two surfaces, the liquid surface tensions, and the interfacial tensions between the liquid, solid, and gas [26]. These three elements interact with each other to achieve equilibrium in the final droplet shape.

The contact angle of a liquid on a GQD's solid surface provides qualitative insights into wettability. In contrast, work of adhesion (W_{SL}) quantitatively measures the energy required to separate the liquid from the solid surface. The contact angle related to interfacial energies of W_{SL} can be calculated using Young - Dupré equation as shown by equation (1) [27]:

$$W_{SL} = \gamma_{LV}(1 + cos\theta) \quad \text{(1)}$$

Where γ_{LV} represents the liquid's surface tension. In this study, water was used as a test liquid and its surface tension at 25°C is 72.8 mN/m [28]. The contact angle, θ is the angle between the tangent of the liquid surface at the contact point and the solid

DOI: https://doi.org/10.11113/jurnalteknologi.v89.24216

surface. The calculated results of the W_{SL} for four concentrations of GQDs sample are tabulated in Table 4.

Table 4 The relation between the contact angle and work of adhesion, W_{SL} for GQDs thin film samples

Sample	Mean Contact Angle (°)	W_{SL} (mN/m)
GQDs1	62.83	106.04
GQDs2	66.57	101.75
GQDs3	36.83	131.07
GQDs4	36.43	131.37

From Table 4, all the GQDs concentrations show high W_{SL}. However, the GQDs3 and GQDs4 exhibit the highest W_{SL} (131.07 and 131.37 mN/m) indicated the strongest liquid to solid adhesion surface. This helps to determine the surface performance in the context of wettability, or compatibility of given liquid.

3.3 ZETA POTENTIAL STABILITY ANALYSIS

In a colloidal solution or dispersion, zeta potential is an essential parameter for the stability of a system in an open environment because the more considerable absolute value of the zeta potential shows a more stable dispersive system. Four different concentrations of GQDs, Figures 6(a) GQDs1, 6(b) GQDs2, 6(c) GQDs3, and 6(d) GQDs4, contributing to the zeta potential plot are shown in Figure 6. The stable GQDs dispersion as measured by the zeta potential, prevent uncontrolled aggregation, provide uniform performance and better interactions with its surroundings. The zeta potential measurements of the GQD's various concentrations are exhibited in Table 5. Zeta potential analysis and contact angle measurement describe understanding interactions between solid-water interfaces. GQDs2 shows the highest absolute zeta potential values of -42.6 mV, suggesting excellent electrostatic stabilization and dispersion uniformity [29]. However, this does not correlate with a higher contact angle of 66.57°, demonstrating moderate hydrophilic concentration compared to other GQDs. The enhancement stability potentially contributed to the improved hydrophilic as observed in higher concentrations of GQDs3 and GQDs4. On the other hand, GQDs1 exhibits the lowest zeta potential values (-15.2 mV), suggesting low electrostatic stabilization, which correlates with a higher contact angle (62.83°) of moderate hydrophilicity.

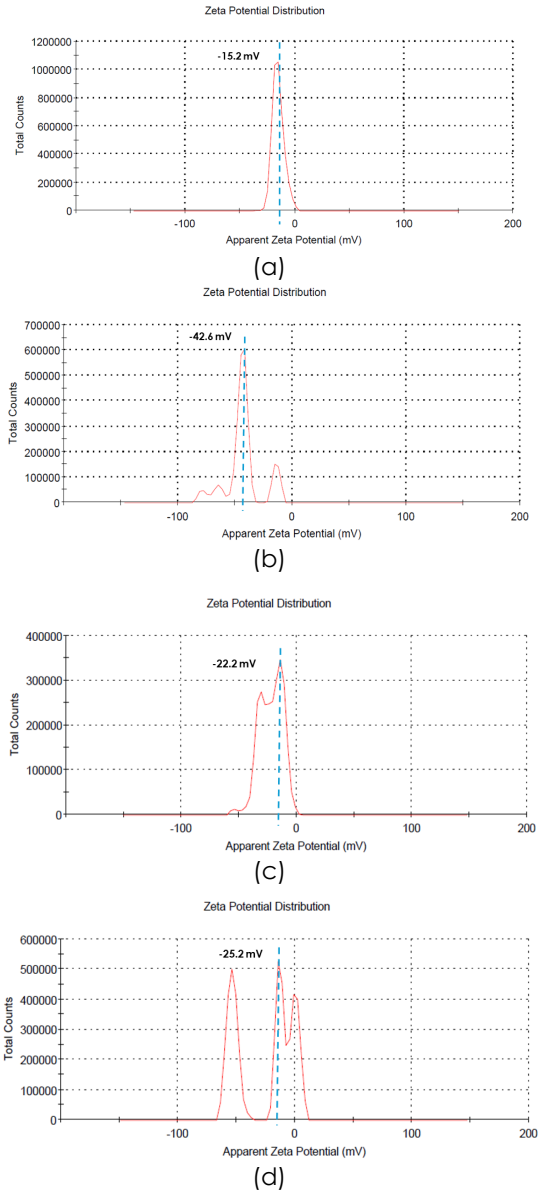


Figure 6 Zeta potential distribution of four different concentrations, (a) GQDs1 (0.1 M), (b) GQDs2 (0.5 M), (c) GQDs3 (1.0 M), and (d) GQDs4 (1.5 M).

Table 5 Zeta potential analysis, contact angle and wettability classification towards GQDs concentrations.

Sample	Zeta Potential Values (mV)	Mean Contact Angle (°)	Wettability Classification
GQDs1	-15.2	62.83	Hydrophilic
GQDs2	-42.6	66.57	Hydrophilic
GQDs3	-22.2	36.83	Hydrophilic
GQDs4	-25.2	36.43	Hydrophilic

This finding aligns with the previous report [30] of transition of water adsorption, which decreases steadily when the dynamic transition surface changes from water-wet to oil-wet states. Interestingly, the anomaly GQDs2 shows an

DOI: https://doi.org/10.11113/jurnalteknologi.v89.24216

unexpectedly high contact angle while the trends suggest higher +/- zeta potential leads to an increase in the hydrophilic state. However, from a study [16], the modified sample from the hydrophilic graphene reveals the most negative zeta potential (-47 mV), indicating the improved hydrophilicity by contact angle indicator (63.9°), improving the dispersion stability due to electrostatic repulsion between particles. The oddity in GQDs2 can be further addressed in the FTIR analysis, revealing the variations and distribution of functional groups on the GQDs surface.

3.4 FOURIER TRANSFORM INFRARED (FTIR) ANALYSIS

In synthesized GQDs, the FTIR analysis supported the observation of the presence of hydroxyl and carbonyl at higher concentrations and improved the surface wettability. Figure 7 shows the FTIR spectra, indicating the stretching vibration of three prominent peaks functional groups in each GQD formation.

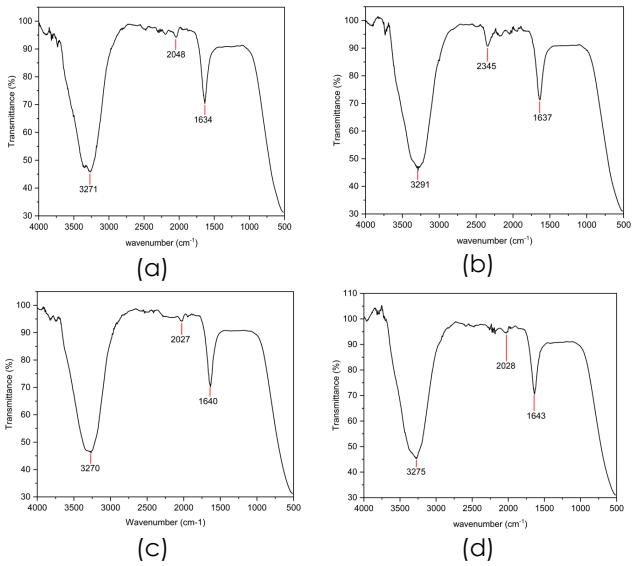


Figure 7 The Fourier transforms infrared (FTIR) analysis of the synthesized GQDs of four different concentrations: (a) GQDs1, (b) GQDs2, (c) GQDs3 and, (d) GQDs4.

The observed peak in the range of 3270 to 3291 cm^{-1} in the concentrations of GQDs corresponds to the vibrations of the hydrogen-bonded hydroxyl group (O—H stretching). This enhances the hydrophilic nature of the GQDs surface. The peak around 1634 to 1643 cm^{-1} is attributed either to the strong carbonyl C=C peak or C=O stretching bonds of carboxylic groups. This shows the existence of π-conjugated domains, a region of molecular structures characterized by alternated single and double bonds that facilitate electron delocalization and carboxylic groups introduced during the hydrothermal treatment. Similarly, a weak peak was observed between 2027 and 2048 cm^{-1} in each GQDs in Figure 5. This absorption may result from overtone vibrations arising from secondary signals due to the molecules absorption of vibration frequencies or minor C≡C stretching modes. On second thought, it could be attributed to the carbon lattice related to the structural characteristics or defects of the carbon framework resulting from the chemical reaction led by the NaOH concentration. Moreover, the presence peak at 2345 cm^{-1} in GQDs is assigned to O=C=O stretching group representing the carbon dioxide (CO_2) that produced during the synthesis. The existence of CO_2 may either be trapped on the surface of the GQDs or intercalated between their layers. However, the carbonate species formed by the reaction of CO_2 on the graphene surface could enhance stability due to the intense negative charge from CO_2 derived groups. Despite the increased stability, the GQDs2 exhibit controlled hydrophilic domains or structural constraints on the surface that limit wettability. These properties make GQDs2 a promising candidate for applications that require a balance between stability and moderate hydrophilicity.

3.5 STRUCTURAL AND COMPOSITIONAL CHARACTERIZATION OF GQDs

In this section, a detailed characterization of GQDs was performed focusing on the GQDs2 sample synthesized at 0.5 M NaOH. This representative sample was selected due to its range spanning the lowest and highest concentrations of NaOH and its relatively stable physicochemical properties during initial testing. The analysis includes ultrahigh-resolution scanning electron microscopy (UHR-SEM), Energy-dispersive X-ray spectroscopy (EDX), Transmission Electron Microscopy (TEM) and X-ray diffraction (XRD) characterizations, all serving as an authorization of the GQDs formation. The comparative results of GQDs1, GQDs3 and GQDs4 highlight the differences in surface wettability and functional behaviour. GQDs2, however, plays a crucial role as a standard prototype to demonstrate the typical features of synthesized GQDs via the hydrothermal treatment method, underlying the importance of the findings.

3.5.1 UHR-SEM AND EDX

The UHR-SEM image illustrates the surface morphology of the GQDs2 sample obtained using a 0.5 M NaOH concentration as shown in Figure 8. At

DOI: https://doi.org/10.11113/jurnalteknologi.v89.24216

the nanoscale, the image appears to be densely packed and well dispersed arrangement of the GQDs indicating a successful formation of a uniform distribution of granular or dot-like features GQDs across the substrate. Importantly, the texture, while appearing roughened, also suggests that the GQDs have been deposited without agglomeration over the substrate.

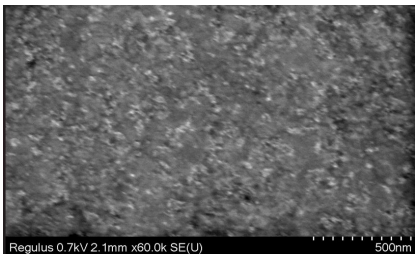


Figure 8 UHR-SEM analysis of the synthesized GQDs2 at the 500nm scale bar.

The EDX elemental analysis presented in Figure 9 confirms the presence of carbon (C), oxygen (O) and sodium (Na) in the synthesized GQDs derived from GO and the reducing agent, NaOH. As shown in Table 6, the oxygen element exhibits the highest weight percentage (51.18%) and atomic percentage (50.5%) indicating the presence of hydroxyl and carbonyl groups as shown in Figure 7. The higher weight percentage (Wt. %) of oxygen compared to carbon (25.24%) validates that the GQDs are highly oxidized, consistent with [31] and [32]. The C:O atomic ratio of 1:1.5 (C) to (O) is suitable for high-functional GQDs. Furthermore, sodium at 23.58 Wt. % (16.21 At. %), was detected alongside carbon and oxygen. The detection of sodium suggests the residual sodium attributed to the NaOH as base catalyst used during hydrothermal synthesized of carbon nanomaterials.

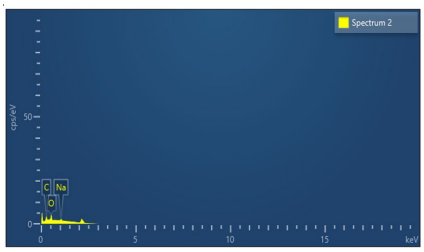


Figure 9 EDX analysis of the synthesized GQDs2

Table 6 The EDX analysis of the synthesized GQDs2

Element	Wt% (Weight%)	Atomic %
C, Carbon	25.24%	33.22%
O, Oxygen	51.18%	50.57%
Na, Sodium	23.58%	16.21%

3.5.2 TEM AND XRD

The morphology of the synthesized GQDs2 was analyzed using a TEM image as shown in Figure 10. The image reveals the presence of dark spots that represent individual GQDs with an average lateral dimension of approximately 3.3 nm. These nearly spherical nanodots are uniformly dispersed across the substrate indicating effective exfoliation of GO. The uniform distribution of these nanosized particles indicates the absence of agglomerates, which suggests good colloidal stability after post-synthesis. This finding supports the potential of stability as discussed in Figure 4(b).

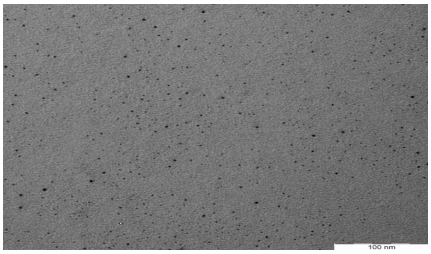


Figure 10: TEM image of the synthesized GQDs at 100nm scale bar

The XRD analysis of the synthesized GQDs derived from GO is illustrated in Figure 11 is a precise investigation into the crystallinity features of the GQDs. GO exhibits a sharp peak at 2θ of 10.4° [32], which shifted to a broad peak centered at 2θ of 19° for a NaOH concentration of 0.5 M corresponding to a (002). This peak indicated the characterization of the amorphous crystalline carbon structures in synthesized GQDs produced via hydrothermal cutting methods. The interlayer d-spacing of GQDs2 was calculated to be 0.467 nm, which is smaller than the d-spacing value of 0.850 nm for GO. This indicates that the GQDs are oxidized only at the edges due to their very small size [32].

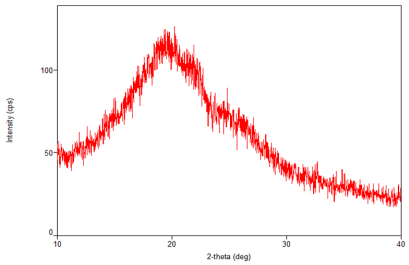


Figure 11: XRD analysis of the synthesized GQDs2

DOI: https://doi.org/10.11113/jurnalteknologi.v89.24216

3.6 EFFECT OF NAOH CONCENTRATION ON GQDS FORMATION MECHANISM

The impact of NaOH concentration on the GO fragmentation can be clarified through observed trends. The concentration of NaOH is a critical factor in the hydrothermal cutting mechanism that facilitates the formation of GO to GQDs. During the hydrothermal reaction, the hydroxide ions (OH^-) interact with oxygen functional groups on GO such as epoxy and hydroxyl groups [33]. As the NaOH concentrations increase, the concentration of OH^- ions during the reaction also increases. This enhancement promotes greater incorporation of oxygen groups on the surface of GQDs.

The interaction between OH^- ions and GO promotes bond cleavage and effectively exfoliates GO into smaller entities of GQDs. Concurrently, OH^- ions contribute to the formation of additional oxygen-containing functional groups on the edge and surface of the GQDs. Higher concentrations of NaOH lead to an increase in the number of polar functional groups formed [34]. Since water is highly adsorbed on surfaces of more polar functional groups, GQDs with a higher density of oxygenated groups exhibit an enhanced hydrophilic nature. A lower contact angle and increased wettability characterized this phenomenon. The trend was consistently observed in GQDs samples, indicating a direct correlation between NaOH concentration and hydrophilic behaviour.

3.7 CORRELATION BETWEEN CONTACT ANGLE, ZETA POTENTIAL AND FTIR ANALYSIS

GQDs surfaces are prone to attracting water molecules, therefore their wettability is key for various applications. The contact angle aims to measure the wetting of condensed water when it encounters different solid surfaces. The wetting properties of a GQD thin film were mainly related to the chemical composition, microstructure, and electric charge on the surface solid. This correlation helps to study the connections with the dynamic changes in surface influenced by the distribution of GQDs and their functional groups.

At lower GQD concentrations (GQDs1 and GQDs2), insufficient hydrophilic functional groups (carboxyl, hydroxyl) attached to the surface lead to a higher contact angle, indicating reduced wettability. However, when the GQD concentration increases (GQDs3 and GQDs4), the density of these functional groups rises, enhancing the hydrophilicity and reducing the contact angle.

The repulsive forces at the liquid-solid interface affect the degree of wettability. The obtained results agree and correlate between the contact angle and zeta potential analysis. The surface of the samples with specific energy tends to attract molecules with similar energy, as in this study, the water shows a negative charge on the surface and is attracted by the GQDs surface. Zeta potential stabilized at higher concentrations, suggesting that the available functional groups are undergoing deprotonation, leading to an increase in negative surface charge density. For graphene-based materials, surface functional groups play an important role in the wettability.

In order to support the dispersion stability analysis, the dispersion of GQDs were characterized by FTIR analysis, which showed the comparison of the exploration of chemical composition of the GQDs due to the presence and density of the surface functional groups on the GQDs coating thin films.

4.0 CONCLUSION

GQDs3 and GQDs4 exhibit strong interactions and adhesion between liquid and solid surfaces. At higher concentrations, a solid surface's resistance being wetted by the test liquid decreases. This behavior is attributed to the higher surface energy of water molecules, which promotes their spreading and maximizes liquid-solid interaction. From the perspective of GQDs cohesion, strong adhesion forces between the surface and water molecules create a large interfacial bond leads the droplet to spread across the surface, resulting in a low contact angle. As the GQDs concentration increases, a lower contact angle indicates the hydrophilicity. The moderate zeta potential of GQDs3 and GQDs4 suggests better hydrophilicity due to higher functional group density. A linear correlation between contact angle and zeta potential has been obtained. However, the anomaly of the GQDs2 finding observed by the FTIR analysis reveals a possible explanation for the correlation. The presence of an O=C=O stretching group, CO_2, indicates greater electrostatic repulsion among particles, resulting in a highly stable suspension. However, the GQDs2 surface has fewer hydrophilic functional groups, reducing its water interaction compared to other GQDs. Despite the high zeta potential stability, the GQDs2 demonstrated a relatively high contact angle and were less hydrophilic than GQDs1, GQDs3, and GQDs4. Yet, the GQDs2 contact angle is within the hydrophilic range.

This study provides a basic understanding of the interaction and wettability of the behavior of GQDs at varying concentrations and the effects of the reagents used during the synthesis of GQDs. The optimization of GQDs concentrations should aim to achieve desired wettability and surface interactions for specific applications such as an antifouling coating, biosensing, and optoelectronics devices. Besides that, focusing on adapting the surface chemistry of GQDs by introducing other functional groups to investigate the influence of contact angle, liquid-solid interaction, and adhesion characteristics of the synthesized GQDs. Finally, conducting a

durability test to evaluate the long-term stability of wettability and zeta potential is crucial for assessing exposure to certain harsh and prolonged conditions, which should also be encouraged.

Acknowledgement

The generous support from Universiti Teknologi MARA (UiTM) and Ministry of Higher Education (MOHE) institutions made this research possible. MOHE funded the project under the Fundamental Research Grant Scheme (FRGS/1/2023/TK07/UITM/02/26) to obtain necessary materials and access to advanced characterization equipment, while UiTM provides necessary facilities.

Conflicts of Interest

The authors declare that there is no conflict of interest regarding the publication of this paper.

Data availability

The data supporting the findings of this study are available from the corresponding author upon reasonable request.

Ethics declaration

Formal ethical approval was not obtained for this study. However, the authors confirm that the research was conducted in accordance with established ethical principles and good research practices, with due consideration given to participant rights, informed consent, confidentiality, and responsible data handling.

References

[1] Anusuya, T., Kumar, V., & Kumar, V. (2021). Hydrophilic graphene quantum dots as turn-off fluorescent nanoprobes for toxic heavy metal ions detection in aqueous media. *Chemosphere*, 282.
DOI : https://doi.org/10.1016/j.chemosphere.2021.131019

[2] Chandrasekaran, R., Uthirakrishnan, U., Sankar, G., Natarajan, K., Joseph, J., & Sagadevan, S. (2024). Recent Progress and Challenges in Graphene Quantum Dots as Multifunctional Nanoplatforms for Biomedical Applications. *BioNanoSci*, 14, 3401-3429.
DOI : https://doi.org/10.1007/s12668-024-01531-9

[3] Li, B., Wang, Y., Huang, L., Qu, H., Han, Z., Wang, Y., Kipper, M. J., Belfiore, L. A., & Tang, J. (2021). Review of performance improvement strategies for doped graphene quantum dots for fluorescence-based sensing. *Synthetic Metals*, 276.
DOI : https://doi.org/10.1016/j.synthmet.2021.116758.

[4] Panachikkool, M., & Pandiyarajan, T. (2024). Graphene quantum dots as game-changers in solar cell technology: a review of synthetic processes and performance enhancement. *Carbon Letters*, 34(1), 445-475.
DOI : https://doi.org/10.1007/s42823-023-00617-w

[5] Liang, Y., Lu, C., Ding, D., Zhao, M., Wang, D., Hu, C., Qiu, J., Xie, G., & Tang, Z. (2015). Capping nanoparticles with graphene quantum dots for enhanced thermoelectric performance. *Chemical Science*, 6(7), 4103-4108.
DOI : https://doi.org/10.1039/c5sc00910c

[6] Santarelli, G., Perini, G., Salustri, A., Palucci, I., Rosato, R., Palmieri, V., Iacovelli, C., Bellesi, S., Sali, M., Sanguinetti, M., De Spirito, M., Papi, M., Delogu, G., & De Maio, F. (2024). Unraveling the potential of graphene quantum dots against Mycobacterium tuberculosis infection. *Frontiers in Microbiology*, 15.
DOI : https://doi.org/10.3389/fmicb.2024.1395815

[7] Cui, Y., Liu, L., Shi, M., Wang, Y., Meng, X., Chen, Y., Huang, Q., & Liu, C. (2024). A Review of Advances in Graphene Quantum Dots: From Preparation and Modification Methods to Application. *C-Journal of Carbon Research*, 10(1).
DOI : https://doi.org/10.3390/c10010007

[8] Bintanel-Cenis, J., Fernández, M. A., Gómara, B., & Ramos, L. (2024). Critical overview on the use of hydrophobic (deep) eutectic solvents for the extraction of organic pollutants in complex matrices. *Talanta*, 270.
DOI : https://doi.org/10.1016/j.talanta.2023.125599

[9] Tie, J., Gao, M., Huang, Y., Li, K., & Wang, H. (2023). Factors influencing wettability and surface/interface mechanics of plant surfaces: a review. *Frontiers in Materials*, 10.
DOI : https://doi.org/10.3389/fmats.2023.1311735

[10] Zhang, C., Wang, X., Li, L., Miller, J. D., & Jin, J. (2024). Surface Wettability Analysis from Adsorption Energy and Surface Electrical Charge. *Minerals*, 14(6).
DOI : https://doi.org/10.3390/min14060628

[11] Vrancken, N., Li, J., Sergeant, S., Vereecke, G., Doumen, G., Holsteyns, F., Chen, C., Terryn, H., De Gendt, S., & Xu, X. M. (2018). In-situ ATR-FTIR for dynamic analysis of superhydrophobic breakdown on nanostructured silicon surfaces. *Scientific Reports*, 8(1).
DOI : https://doi.org/10.1038/s41598-018-30057-w

[12] Griffo, R., Di Natale, F., Minale, M., Sirignano, M., Parisi, A., & Carotenuto, C. (2024). Analysis of Carbon Nanoparticle Coatings via Wettability. *Nanomaterials*, 14(3).
DOI : https://doi.org/10.3390/nano14030301

[13] Serrano-Lotina, A., Portela, R., Baeza, P., Alcolea-Rodriguez, V., Villarroel, M., & Ávila, P. (2023). Zeta potential as a tool for functional materials development. *Catalysis Today*, 423.
DOI : https://doi.org/10.1016/j.cattod.2022.08.004

[14] Cottet, J., Oshodi, J. O., Yebouet, J., Leang, A., Furst, A. L., & Buie, C. R. (2023). Zeta potential characterization using commercial microfluidic chips. *Lab on a Chip*, 24(2), 234-243.
DOI : https://doi.org/10.1039/d3lc00825h

[15] Rodriguez-Loya, J., Lerma, M., & Gardea-Torresdey, J. L. (2024). Dynamic Light Scattering and Its Application to Control Nanoparticle Aggregation in Colloidal Systems: A Review. *Micromachines*, 15(1).
DOI : https://doi.org/10.3390/mi15010024

[16] Cao, L., Li, Z., Su, K., & Cheng, B. (2016). Hydrophilic Graphene Preparation from Gallic Acid Modified Graphene Oxide in Magnesium Self-Propagating High Temperature Synthesis Process. *Scientific Reports*, 6.
DOI : https://doi.org/10.1038/srep35184

[17] Wciślik, S., & Mukherjee, S. (2022). Evaluation of three methods of static contact angle measurements for TiO2nanofluid droplets during evaporation. *Physics of Fluids*, 34(6).
DOI : https://doi.org/10.1063/5.0096644

[18] Chau, T. T. (2009). A review of techniques for measurement of contact angles and their applicability on mineral surfaces. *Minerals Engineering*, 22(3), 213-219.
DOI : https://doi.org/10.1016/j.mineng.2008.07.009

[19] Law, K.-Y., & Zhao, H. (2016). Contact Angle Measurements and Surface Characterization Techniques. In Surface Wetting (pp. 7-34). *Springer International Publishing*.
DOI : https://doi.org/10.1007/978-3-319-25214-8_2
[20] Alina Peethan, M. Aravind, & Sajan Daniel George. (2023). Surface Wettability and Superhydrophobicity. In Advances in Superhydrophobic Coatings (pp. 1-25). *Royal Society of Chemistry*.
DOI : https://doi.org/10.1039/9781837670031-00001
[21] Webb, H. K., Crawford, R. J., & Ivanova, E. P. (2014). Wettability of natural superhydrophobic surfaces. *Advances in Colloid and Interface Science*, 210, 58-64.
DOI : https://doi.org/10.1016/j.cis.2014.01.020
[22] Heib, F., & Schmitt, M. (2016). Statistical contact angle analyses with the high-precision drop shape analysis (HPDSA) approach: Basic principles and applications. *Coatings*, 6(4).
DOI : https://doi.org/10.3390/coatings6040057
[23] Beketov, G. V., & Shynkarenko, O. V. (2022). SURFACE WETTING AND CONTACT ANGLE: BASICS AND CHARACTERISATION. *Himia, Fizika Ta Tehnologia Poverhni*, 13(1), 3-35.
DOI : https://doi.org/10.15407/hftp13.01.003
[24] Hejda, F., Solař, P., & Kousal, J. (2010). Surface Free Energy Determination by Contact Angle Measurements-A Comparison of Various Approaches. *WDS' 10 Proceedings of Contributed Papers*, Part III, 25-30.
[25] Manuel Palencia. (2017). Surface free energy of solids by contact angle measurements. *Journal of Science with Technological Applications*, 2, 84-93.
DOI:https://doi.org/10.34294/j.jsta.17.2.17
[26] Sadullah, M. S., Xu, Y., Arunachalam, S., & Mishra, H. (2024). Predicting droplet detachment force: Young-Dupré Model Fails, Young-Laplace Model Prevails. *Communications Physics*, 7(1).
DOI : https://doi.org/10.1038/s42005-024-01582-0
[27] Nagy, N. (2024). Determination of solid-liquid adhesion work on flat surfaces in a direct and absolute manner. *Scientific Reports*, 14(1).
DOI : https://doi.org/10.1038/s41598-024-81710-6
[28] Kozbial, A., Li, Z., Conaway, C., McGinley, R., Dhingra, S., Vahdat, V., Zhou, F., Durso, B., Liu, H., & Li, L. (2014). Study on the surface energy of graphene by contact angle measurements. *Langmuir*, 30(28), 8598-8606.
DOI : https://doi.org/10.1021/la5018328
[29] Deng, D., Meng, H., Ma, Y., Guo, Y., Wang, Z., He, H., Liu, J. E., & Zhang, L. (2022). Effects of extracellular polymeric substances on the aggregation of Aphanizomenon flos-aquae under increasing temperature. *Frontiers in Microbiology*, 13.
DOI : https://doi.org/10.3389/fmicb.2022.971433
[30] Bassioni, G., & Taha Taqvi, S. (2015). Wettability studies using zeta potential measurements. *Journal of Chemistry*, 2015.
DOI : https://doi.org/10.1155/2015/743179
[31] Mukherjee, D., Das, P., Kundu, S., & Mandal, B. (2022). Engineering of graphene quantum dots by varying the properties of graphene oxide for fluorescence detection of picric acid. *Chemosphere*, 300.
DOI : https://doi.org/10.1016/j.chemosphere.2022.134432
[32] Nair, R. V., Thomas, R. T., Sankar, V., Muhammad, H., Dong, M., & Pillai, S. (2017). Rapid, Acid-Free Synthesis of High-Quality Graphene Quantum Dots for Aggregation Induced Sensing of Metal Ions and Bioimaging. *ACS Omega*, 2(11), 8051-8061.
DOI : https://doi.org/10.1021/acsomega.7b01262
[33] Eigler, S., Grimm, S., Hof, F., & Hirsch, A. (2013). Graphene oxide: A stable carbon framework for functionalization. *Journal of Materials Chemistry A*, 1(38), 11559-11562.
DOI : https://doi.org/10.1039/c3ta12975f
[34] Danushika, G., Yap, P. L., & Losic, D. (2025). Graphene Innovation and Technology Oxygen Functional Groups in Graphene Oxide Using Titration Methods: Quantitative Analysis and New Quality Parameters. *Graphene Innovation and Technology*, 1(1), 3.